Current Synthetic and Systems Biology
ISSN: 2332-0737

Murabito, Curr Synthetic Sys Biol 2013, 1:1
DOI: 10.4172/2332-0737.1000104

Research Article Open Access

Targeting Breast Cancer Metabolism: A Metabolic Control Analysis Approach

Ettore Murabito*

Manchester Centre for Integrative Systems Biology, Manchester Institute of Biotechnology, The University of Manchester, United Kingdom

Abstract

In many diseases, such as cancer, cells show a specific metabolic shift from their normal physiological state. The differences between the normal and the altered metabolic phenotypes may be exploited to identify points of fragility characterising the disease, and hence to specifically target altered cells. The application of Metabolic Control Analysis (MCA) has been proposed as a possible way to identify such points of fragility at the metabolic level. Here we use an MCA approach to assess the suitability of different enzymes as molecular targets for drugs designed to attack breast cancer. We base our study on experimental data characterising the metabolic features of breast cancer, and make use, where possible, of actual kinetic equations in the attempt to provide the most realistic description of the system under study. Unknown metabolic and kinetic quantities are sampled randomly, providing us with a probabilistic assessment of the control profile of the system in the two metabolic phenotypes. The suitability of the different enzymes as molecular targets is subsequently assessed with respect to criteria of both high efficacy and low toxicity.

Keywords: Computational medicine; Systems medicine; Cancer; Metabolic control analysis; Network drug design

Introduction

For almost a century, it has been known that the emergence of cancer is accompanied by specific metabolic alterations. In particular, most cancer cells are characterized by increased glucose consumption and an aerobic glycolytic activity (known as the Warburg effect) [1]. This metabolic shift, observed almost universally during carcinogenesis, has always been considered a reliable biomarker for tumours [2], and today researchers are assessing the possibility to exploit it in order to target cancer cells more specifically than through traditional approaches [3]. There is currently a quest to find anticancer drugs operating at the metabolic level with both high efficacy and low toxicity. The underlying idea consists of identifying enzymes that represent points of fragility that specifically characterise the cancerous metabolic phenotype [4-6]. These enzymes are such that an alteration in their activity (due for example to the action of an anticancer drug) would elicit the desired response in cancer cells, without affecting their normal counterparts. Metabolic Control Analysis (MCA) is a conceptual framework that can profitably be used to identify such points of fragility [7-9]. The aim of MCA is to understand how the control upon a system's property is distributed among the different enzymatic steps of a metabolic network [7]. Enzymes which exert a strong control over a property of interest in the cancer metabolic phenotype and a low control in the normal phenotype can be considered good candidate targets for a drug aimed to elicit a high differential response between neoplastic and normal cells.

One way to apply MCA and gain insights on the suitability of the different enzymes as putative molecular targets is to generate a fully characterized computational representation of the system under study [10]. Unfortunately, a complete dynamic characterization of a metabolic network is often hindered by the lack of data about the kinetic mechanism of the different enzymatic steps and the value of many parameters to the relevant *in vivo* conditions. A possible way to circumvent this limitation consists of sampling the uncertain or unknown quantities and predicting the control properties of the system on a probabilistic basis [11-17]. In a previous work [18] we showed how putative targets for drugs operating at the metabolic level may be identified through MCA in a probabilistic manner, when minimal knowledge is available about the dynamic properties of the system. In particular we showed that the complete set of fluxes and concentrations defining the two metabolic states under comparison, combined with heuristic assumptions on the properties of typical enzyme- catalysed reactions, already allows for a fast and efficient way to explore the effectiveness of putative drug targets in the abundant cases where detailed kinetic models are unavailable or incomplete. In that work our methodology was applied as a proof-of-concept to show how points of fragility characterizing a paradigmatic cancer metabolic phenotype can be identified, while using only generalised Michaelis-Menten equations to describe the kinetics of the different enzymatic steps. Here we apply the same conceptual framework to address a similar issue but with a more specific clinical implication. In particular, we aim to assess the suitability of different metabolic enzymes as putative molecular targets for a drug specifically designed to attack breast cancer. The present work builds on existing knowledge of the system's metabolic physiology and the kinetic properties of the different reaction steps. We based our study on the experimental data currently available in the literature about the metabolic features of breast cancer, and made use, wherever possible, of actual kinetic equations in the attempt to minimize the uncertainty introduced in the description of the system dynamics. The reason for choosing this type of cancer lies on the fact that breast cancer is, to our knowledge, the most extensively characterized in terms of the pattern of the metabolic fluxes acquired by the cells during carcinogenesis and some of the metabolite concentrations [19,20]. The uncertainties of the system, such as unknown parameter values or unquantified metabolite concentrations, are randomly sampled allowing for a probabilistic assessment of how the control profile of the system differs between the two metabolic states: cancer and normal. These differences are then used to identify the best putative enzyme targets with respect to specific

***Corresponding author:** Ettore Murabito, Manchester Centre for Integrative Systems Biology, Manchester Institute of Biotechnology, The University of Manchester, United Kingdom, Tel: +44 306 5146; E-mail: Ettore.Murabito@manchester.ac.uk

Received July 05, 2013; **Accepted** August 19, 2013; **Published** August 22, 2013

Citation: Murabito E (2013) Targeting Breast Cancer Metabolism: A Metabolic Control Analysis Approach. Curr Synthetic Sys Biol 1: 104. doi: 10.4172/2332-0737.1000104

clinical strategies aimed to attack breast cancer cells in an effective and non- toxic way.

Methods

MCA to locate points of fragility of a metabolic system

The concept of control coefficient is central in MCA and provides a way to evaluate – at steady-state – the extent to which a property of interest changes in response to a perturbation in the activity of an enzyme [7,21,22]. Important examples of control coefficients are the flux control coefficient C_i^J and the concentration control coefficient C_i^S, defined as

$$C_i^J := \lim_{\Delta v_i \to 0} \frac{\Delta J/J}{\Delta v_i/v_i} = \frac{dJ/J}{dv_i/v_i} = \frac{d\ln(J)}{d\ln(v_i)} \quad (1)$$

$$C_i^S := \lim_{\Delta v_i \to 0} \frac{\Delta S/S}{\Delta v_i/v_i} = \frac{dS/S}{dv_i/v_i} = \frac{d\ln(S)}{d\ln(v_i)} \quad (2)$$

where J is the steady-state flux of a given pathway, S the steady-state concentration of a given metabolite and v_i is the catalytic activity of enzyme i. In Eqs. (1) and (2) it is assumed that the change in the enzymatic activity v_i (which elicits changes in steady-state fluxes and concentrations) is caused by the action of an effector (for example a drug) acting directly and selectively on the enzymatic step i. Given a metabolic state $\left(\mathbf{v}^0, \mathbf{S}^0\right)$, described in terms of the complete set of fluxes and metabolite concentrations at steady-state, Reder [23] showed that the matrix of the flux control coefficients $\mathbf{C}^J$ and the matrix of the concentration control coefficients $\mathbf{C}^S$ may be expressed as

$$\mathbf{C}^S = -\left(\mathbf{D}_{\mathbf{S}^0}\right)^{-1} \cdot \mathbf{L} \cdot \left(\mathbf{N} \cdot \left.\frac{\partial \mathbf{v}}{\partial \mathbf{S}}\right|_0 \cdot \mathbf{L} \right)^{-1} \cdot \mathbf{N} \cdot \mathbf{D}_{\mathbf{v}^0} \quad (3)$$

$$\mathbf{C}^J = \mathbf{1} + \mathbf{D}_{\mathbf{v}^0}^{-1} \cdot \left.\frac{\partial \mathbf{v}}{\partial \mathbf{S}}\right|_0 \cdot \mathbf{D}_{\mathbf{S}^0} \cdot \mathbf{C}^S \quad (4)$$

where $\mathbf{D}_{\mathbf{v}^0}$ and $\mathbf{D}_{\mathbf{S}^0}$ denote diagonal matrices of elements $\mathbf{S}^0$ and , while $\mathbf{N}'$ and $\mathbf{L}$ denote respectively the reduced stoichiometric matrix and the link matrix (see [23] for definitions), both completely determined by the stoichiometry of the system.

Here we use Eqs. (3) and (4) to evaluate the control properties of the system under two different metabolic states, one representing the cancerous phenotype and the other representing the normal phenotype. The information needed to evaluate the control coefficients cover the stoichiometry of the system (given by $\mathbf{N}'$ and $\mathbf{L}$), its dynamic properties (reflected in the partial derivatives $\partial\mathbf{v}/\partial\mathbf{S}$) and the two sets of fluxes and metabolite concentrations defining the two metabolic states (as described by $\mathbf{D}_{\mathbf{v}^0}$ and $\mathbf{D}_{\mathbf{S}^0}$). We base this information as much as possible on literature data in an attempt to minimize uncertainties in the definition of the system properties and the metabolic states under comparison. As we will see later in this section, unknown or uncertain quantities such as kinetic parameters or some of the metabolite concentrations are sampled from reasonable ranges of values.

Definition of the metabolic map

The system under study is a representation of the central carbon metabolism as depicted in Figure 1, and consists of glycolysis, the pentose phosphate pathway, the TCA cycle and a simplified representation of the respiratory chain.

Three different compartments are taken into account: the cytosol, hosting glycolysis and the pentose phosphate pathway; the mitochondria, where the TCA cycle takes place; and the intermembrane space, where the protons produced in mitochondria are pumped in and subsequently released from for the mitochondrial synthesis of ATP. We note that considering the intermembrane space adds an unnecessary degree of details to our representation of central carbon metabolism, as protons equilibrate immediately between intermembrane space and cytosol. However, we chose to consider explicitly all the three compartments to provide a better schematic representation of the system under study.

Our model represents an extension of the reconstruction of erythrocyte central carbon metabolism by Schuster and Holzhütter [24]. The choice to adopt the latter model as our starting point was motivated by the fact that erythrocyte metabolism is the most extensively studied and characterized. Schuster and Holzhütter's model, in particular, provides us with a detailed description of the kinetics of each enzymatic step and a comprehensive regulatory map of the metabolic regulations occurring in glycolysis as well as in the pentose phosphate pathway. Additional reactions were added to this initial model in order to take into account the TCA cycle and the oxidative phosphorylation, which are absent in human erythrocytes. The ANT

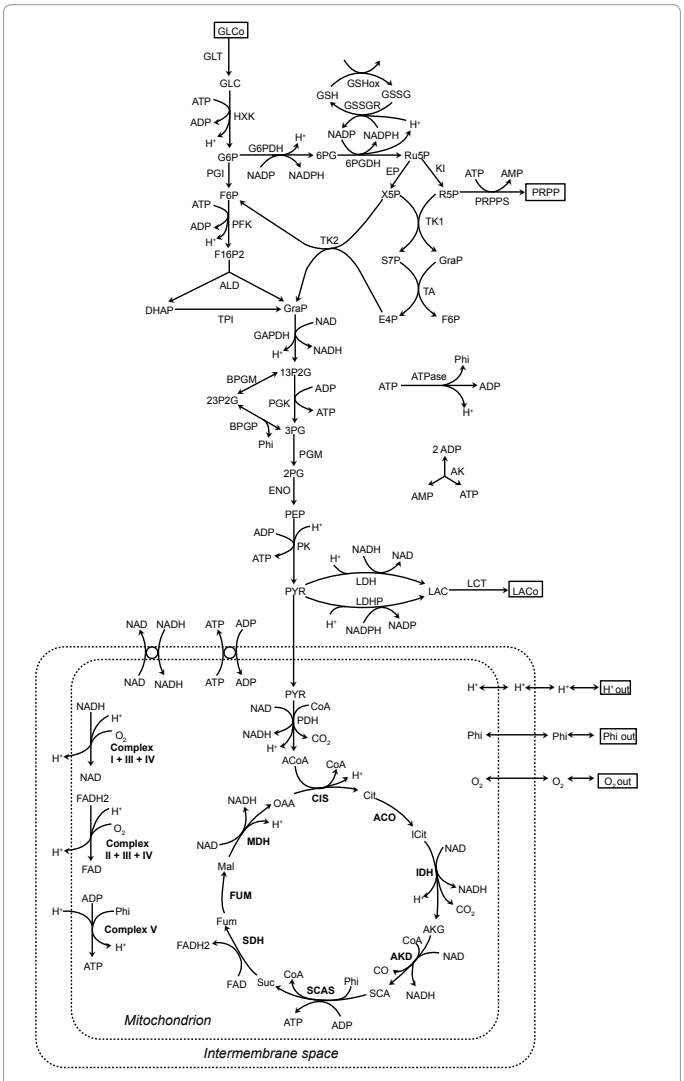

Figure 1: Metabolic map of central carbon metabolism. The pathways and metabolic processes taken into account are glycolysis, the pentose phosphate pathway, the TCA cycle and a simplified representation of the oxidative phosphorylation.

transporter and a phenomenological translocation step accounting for the shuttling activity of NAD/NADH were also introduced to connect the cytoplasm to the mitochondria.

Following Li et al. [25], the electron transport chain and oxidative phosphorylation are described through three lumped reactions (see Supplementary Material for details).

Rate laws of the reaction steps

The enzyme kinetics of glycolysis and the pentose phosphate pathway is described through the same rate equations used in Schuster's reconstruction of erythrocyte central carbon metabolism [24]. With respect to a generic biochemical reaction $\alpha_1 A_1 + \alpha_2 A_2 + \ldots \rightarrow \beta_1 B_1 + \beta_2 B_2 + \ldots$, all these equations can be written in the following general form [24]:

$$v = V_{\max} \cdot \left(\Pi_k A_k^{\alpha_k} - \frac{\Pi_l B_l^{\beta_l}}{K_{eq}} \right) \cdot f(\mathbf{A}, \mathbf{B}, \mathbf{E}, \mathbf{K}) \quad (5)$$

where K_{eq} denotes the equilibrium constant, $V_{\max}$ the maximal forward rate, and f is a function containing all the non-linearities due to saturation, allostery, etc. This function depends on the concentrations of reactants (**A**), products (**B**) and effectors (**E**), and on the kinetic parameters (**K**) such as Michaelis constants or activation/inhibition constants. The benefit of using reaction rates that can be expressed through the general form of Eq. (5) is that the thermodynamic properties, described by the factor $\left(\Pi_k A_k^{\alpha_k} - \Pi_l B_l^{\beta_l} / K_{eq} \right)$ are maintained separated from the specific enzymatic mechanism governing the reaction dynamics. In expanding Schuster and Holzhütter's model to encompass the respiration pathway, we tried to describe the kinetics of the reactions in the TCA cycle following this same principle. The rate equations, in particular, were taken from Wu et al. [26] (for PDH, CIS, ACO, IDH and AKD) and Mogilevskaya et al. [27] (for SDH and FUM). The kinetics of SCAS and MDH were described in terms of generalized Michaelis-Menten rate laws, in the specific implementation proposed by Liebermeister and Klipp [28].

The kinetics of the three lumped reactions representing the electron chain and oxidative phosphorylation were described through the same rate laws used in Li et al. [25], where the general form of Eq. (5) is modified in order to take into account the dependency of the reaction rates on the proton motive force (see Supplementary Material for details).

The intercompartment translocation of metabolites depends on the action of specific carriers. The kinetics of carrier mediated transport was described through the general rate equation proposed by Li et al. [25]. For the facilitated translocation of an uncharged metabolite S from compartment $c1$ to compartment $c2$, this rate equation can be written as follows:

$$v = T_{\max} \left(\frac{S_{c1}}{K_M + S_{c1}} - \frac{S_{c2}}{K_M + S_{c2}} \right) \quad (6)$$

where S_{c1} and S_{c2} denote the concentrations of S in compartment $c1$ and $c2$ respectively, T_{max} is the maximal transport rate from compartment $c1$ to compartment $c2$, and K_M is the Michaelis-Menten constant. A modified version of of Eq.(6) was used to describe the translocation of ATP/ADP via ANT and the apparent transport of NAD/NADH between cytosol and mitochondria in order to take into account the effect of the mitochondrial membrane potential on these charged cofactors (details given in Supplementary Material).

The non facilitated transport was described through a passive diffusion rate equation:

$$v = \lambda (S_{c1} - S_{c2}) \quad (7)$$

where λ is the permeability coefficient for diffusion from $c1$ to $c2$.

Defining the metabolic states under comparison

The normal phenotype: Schuster and Holzhütter's model of erythrocyte metabolism was used as starting point not only for the creation of the metabolic map depicted in Figure 1, but also in the definition of the normal metabolic state. In particular, its metabolite concentrations were used as representative of typical physiological values. The pattern of fluxes through the different branches was also maintained as in Schuster and Holzhütter's [24] original model, with the exception of the lactate dehydrogenase flux, which was mainly diverted toward the TCA cycle in order to represent the functioning of a normal cell, where glucose is processed through the respiration pathway. To evaluate the fraction of glycolytic flux entering the TCA cycle, the rates of glucose uptake and lactic acid secretion are set to the physiological value measured in skeletal muscle cells at normal resting condition, respectively 0.195 and 0.09 mM/min [25]. To accomplish this, we rescale the fluxes through glycolysis and the pentose phosphate pathway in order to preserve the original flux distribution pattern, (i.e. the fluxes maintain the same relative value with respect to each other). The flux entering the TCA cycle has been obtained by subtracting the conversion rate of pyruvate into lactate from the pyruvate kinase flux, thus ensuring the mass balance of pyruvate at steady-state.

By allowing the flux from pyruvate to enter the TCA cycle, the oxidation of NADH into NAD through lactate dehydrogenase can only occur at a lower rate than in the complete fermentative regime of Shuster and Holzhütter's model, thus breaking the original redox balance in the cytosol. The rate of NAD-NADH translocation between cytosol and mitochondria was set to restore this balance, while maintaining the original cytosolic concentration of the two cofactors. This translocation step was introduced to represent the transport of NAD and NADH via the glutamate-aspartate cycle and the glycerol phosphate cycle. The net production and transportation rate of NADH in and toward mitochondria was in turn counterbalanced by the reduction of NADH into NAD in the electron transport chain and oxidative phosphorylation, where mitochondrial ADP is phosphorylated to ATP. The balance between mitochondrial ADP and ATP was maintained by allowing the ATP produced in the oxidative phosphorylation to be released in the cytosol, while importing an equal amount of cytosolic ADP into mitochondria.

Disease phenotype: To our knowledge, no study has been performed yet that characterizes the metabolic cancer phenotype in terms of both fluxes and metabolite concentrations. For a partial characterization of the cancerous metabolic phenotype we used the pattern of fluxes measured by Richardson et al. [19] in the most advanced stage of tumour progression in breast cancer. This pattern of fluxes is characterized by a different distribution of the glucose uptake flux amongst the different pathways of the central carbon metabolism. In particular, the flux entering the pentose phosphate pathway now accounts for ~26% of the pyruvate production versus the 2% of the normal metabolic state.

The analysis of Richardson et al. [19], based on ^{13}C labelling techniques, implies the quantification of specific metabolites as a prerequisite to assess the downstream trafficking of carbon influx. However, the set of metabolites for which the concentration is provided in their study do not overlap with the metabolic intermediates of

glycolysis, pentose phosphate pathway and TCA cycle, as depicted in Figure 1 (the only exceptions are lactate and succinate). Moreover, the concentrations are given in terms of relative changes between the least and most advanced stages of cancer progression considered in their study, making them unsuitable for retrieving absolute concentrations starting from a normal metabolic phenotype.

Some of the concentrations of glycolytic intermediates, however, can be retrieved from earlier studies. Cohen et al. [20], for example, quantified the differences in the phosphate metabolite levels in a number of breast cancer cell lines, thus providing us with a range of values that can be used to constrain some of the glycolytic intermediate concentrations. Some general features of cancer physiology can also help us to reduce the uncertainty in the characterization of the cancerous metabolic profile. For example, lactate is generally found to be present in tumours at levels much higher than in the corresponding normal tissues [29-32]. On the other hand, despite the increased acid production, different studies have consistently demonstrated that the intracellular pH of tumours is the same or slightly alkaline compared with that of normal cells [33], as tumour cells excrete protons through up-regulation of the Na^+/H^+ antiport and other membrane transporters. Consequently, extracellular pH is substantially lower (usually by ~0.5 pH unit) than normal [34-36]. Some other constraints may be inferred through some general considerations. For example, in normal cells, as a consequence of the activity of the respiration chain and the coupled ATP synthesis, pH in mitochondria is higher than in cytosol. On the other hand, in the absence of any respiration activity the proton concentration in mitochondria cannot exceed the proton concentration in cytosol. This provides us with a lower and upper bound for the mitochondrial pH in cancer cells, where the respiratory activity, relative to the glucose uptake, is lower than it would be in a full respiratory regime. Table 1 lists the range of values we set for some of the metabolic intermediates in the cancerous phenotype and the corresponding bibliographic references (as numbered in the main article).

Sampling metabolite concentrations

The uncertainty in the definition of the cancerous phenotype due to the lack of unique values for most of the metabolite concentrations has an effect on the outcome of the system in terms of its control profile. This effect was assessed through a random sampling approach, where the uncertain metabolite concentrations were sampled and the control coefficients subsequently evaluated.

Sampling metabolite concentrations in a sensible manner is not trivial. These concentrations have to satisfy the thermodynamic constraints imposed by the reactions in which the corresponding metabolites are involved and the set of steady-state fluxes characterizing the metabolic state under consideration. The rate equations used in our model are such that the logarithmic form of the corresponding thermodynamic constraints can be expressed as linear inequalities

$$\sum_{i=1}^{m} N_{ij} X_i \lessgtr b_j \text{ with j=1,2,..n} \quad (8)$$

where X_i is the logarithmic concentration of metabolite S_i and N_{ij} is the stoichiometric coefficient of S_i in reaction j. The direction of the inequalities in Eq. (8) depends on the specific reaction j, and is determined in particular by the sign of the flux at steady-state and the specific rate equation from which the constraint is derived. For the metabolite concentrations to be thermodynamically meaningful, their logarithmic values have to satisfy simultaneously all the n linear inequalities of Eq. (8). To sample values which are compliant with this requirement, we used the known property according to which, given a set of solutions $\{\mathbf{X}^{(1)}, \mathbf{X}^{(2)},\ldots, \mathbf{X}^{(K)}\}$ of Eq. (8), any linear combination of the form

$$\frac{\sum_{k=1}^{k} \varphi_k \mathbf{X}^{(k)}}{\sum_{k=1}^{k} \varphi_k} \quad (9)$$

is also a solution of the same set of inequalities. Thanks to this property, once an initial representative set of solutions is found, a thermodynamically compliant way to sample the metabolite concentrations consists of combining these solutions linearly with random coefficients φ_k. To find a first representative set of solution $\{\mathbf{X}^{(1)}, \mathbf{X}^{(2)},\ldots, \mathbf{X}^{(K)}\}$ we used a linear programming approach, in the form of the algorithm proposed by Lee et al. [38]. More details are provided in Supplementary Materials.

Metabolite	Range of values	Reference
Glucose (Glc)	0.05–0.95	[37]
Glucose-6-phosphate (G6P)	0.0153–0.90 (a)	[20]
Fructose-6-phosphate (F6P)	0.0765–1.131 (a)	[20]
GSH	0.4–2.3	[37]
Lactic acid (Lac)	5.02–10.7	[29-32,37]
Succinate (Succ)	0.9–3.2 (b)	[37]
pH (cytosol)	7.1	[33]
pH (mitochondria)	<7.6; >7.1	

(a) The concentration of G6P and F6P were originally expressed in μmol/10^8 cells. To convert these values to mM, we evaluated the cellular volume assuming spherical cells of typical diameter 50 μm.
(b) The original values refer to the concentration of succinate with respect to the total cell volume. To convert those values to mitochondrial concentrations, we multiply them by a factor of 10.

Table 1: List of constraints for metabolite concentrations in the cancerous phenotype.

Sampling kinetic parameters

Another source of uncertainty is represented by the value of the kinetic parameters. As a reference point we adopted the parameter values originally used in the publications from which the kinetic equations were taken. However one needs to be aware that the values of kinetic parameters are often retrieved by fitting a model to the experimentally observed behaviour of the system under study. Partial knowledge of the enzymatic mechanisms or simplifying assumptions on the topology of the network or its regulatory map may cause the fitted kinetic parameters to differ appreciably from their *in vivo* value. Because of these reasons we also considered the kinetic parameters among the quantities to be sampled with the aim to assess to what extent their precise value is relevant in determining the control profile of the system. From an operational standpoint, we distinguish between different kinds of parameters:

1. The equilibrium constants K_{eq} were taken from Holzhütter [39] for all the reactions and assumed to be known.

2. Affinity, inhibition or activation constants were sampled randomly. The sampling was performed logarithmically and covered, for each parameter, two orders of magnitude around its original value (i.e. the value provided in the work from which the corresponding kinetic law was taken).

3. Maximal activities such as V_{max} and T_{max} were adjusted at each sampling iteration in order to make the metabolic state (i.e. metabolite concentrations and fluxes) compliant with the steady-state condition.

With reference to the generic rate law in Eq. (5) as an example, the

concentrations of the reactants (**A**), products (**B**) and effectors (**E**) of a given reaction, as well as its flux v, are defined by the metabolic state under consideration (either the normal or the cancerous state) and are assumed to be known. When the concentration of a specific metabolite is uncertain, then it is sampled as explained earlier. Either way, knowledge of the metabolite concentrations, fluxes and equilibrium constants is prior to the parameter sampling. Once the affinity, inhibition and activation constants (**K**) are sampled, the rate equation is reversed with respect to V_{max}, and the maximal activity evaluated. This allows us to have a set of sampled parameter that, together with the maximal activity, is compliant with the state-state condition.

Identifying putative drug targets

The suitability of the different enzymes as putative drug targets was assessed with respect to the same three criteria used in our previous work [18]. We briefly summarise them here. In doing so we assume that the aimed action of a drug hitting an enzyme i is meant to induce a decrease in a given flux J_{target}.

Maximal selectivity: The selectivity coefficient

$$S_i^{J_{target}} \equiv C_{i(\text{cancer})}^{J_{target}} - \left| C_{i(\text{normal})}^{J_{target}} \right| \tag{10}$$

was used to quantify the differential response of the system in the two metabolic states under comparison, cancer and disease. Here $C_{i(\text{cancer})}^{J_{target}}$ and $C_{i(\text{normal})}^{J_{target}}$ denote the control coefficients of enzyme i with respect to J_{target} in the cancer and normal metabolic state respectively. The higher the (positive) value of $S_i^{J_{target}}$ the higher the differential response elicited by a drug hitting enzyme i. We are interested in enzymes with the highest possible value of $S_i^{J_{target}}$, where the average is computed over all the sampling iterations.

Minimal toxicity: The toxicity coefficient T_i

$$T_i = \frac{1}{N} \sum_j \left| C_{i(\text{normal})}^{J_{target}} \right| \quad j \in \{ \text{all the N exchange fluxes} \} \tag{11}$$

was used to assess to which extent perturbations in the activity of enzyme i affect the overall behaviour of the system in the normal metabolic state. The propensity of the system to move away from its original status due to the action of a drug hitting enzyme i is measured through the average sensitivity of the input and output of the system with respect to catalytic activity of that enzyme. The requirement of low toxicity translates into low values of $\overline{T_i}$.

Maximal reliability: The reliability of the calculated average selectivity $\overline{S_i^{J_{target}}}$ was evaluated through the reliability coefficient, defined as:

$$R_i^{J_{target}} \equiv \frac{\overline{S_i^{J_{target}}}}{\sigma\left(S_i^{J_{target}}\right)} \tag{12}$$

where $\sigma\left(S_i^{J_{target}}\right)$ denotes the standard deviation of the calculated selectivities over all the sampling iterations.

To make the three criteria above quantitatively comparable, we normalized the three coefficients defined in Eq. (10), (11) and (12) as follows:

$$\sigma_i \equiv \frac{\overline{S_i^{J_{target}}}}{\max_{\text{all}i}\left\{\overline{S_i^{J_{target}}}\right\}} \tag{13}$$

$$\rho_i \equiv \frac{\overline{R_i^{J_{target}}}}{\max_{\text{all}i}\left\{\overline{R_i^{J_{target}}}\right\}} \tag{14}$$

$$\frac{1}{\tau_i} = \frac{\max\left\{\overline{T_i}\right\} - \overline{T_i}}{\max\left\{\overline{T_i}\right\} - \min\left\{\overline{T_i}\right\}} \tag{15}$$

When considering only enzymes with positive $\overline{S_i^{J_{target}}}$, all the three normalized coefficients have values spanning from 0 to 1. Here 0 represents the worst scenario in terms of either selectivity (normal and cancer cells are equally responsive in magnitude), toxicity (highest alteration of the normal metabolic phenotype) and reliability (maximal uncertainty of the average selectivity). On the other end, 1 represents the best possible result for all the three criteria. We used the normalized coefficients σ_i, $1/\tau_i$, ρ_i to compute, for each enzyme i, a unique score Z_i accounting simultaneously for all the three criteria mentioned above:

$$Z_i = \frac{w_\sigma \cdot \sigma_i + w_\rho \cdot \rho_i + \frac{w_\tau}{\tau_i}}{w_\sigma + w_\rho + w_\tau} \tag{16}$$

where w_σ, w_ρ and w_τ are weight factors that can be chosen according to the specific relation of priority one wants to give to the three criteria.

Results

Different strategies for targeting cancer metabolism

The results reported in this section refer to three possible strategies of intervention to target cancer metabolism.

• Strategy 1 – The first strategy consists of blocking glucose uptake in an attempt to starve cancer cells specifically. Because of the high dependence of cancer cells on glucose as source of energy [40], decreasing the glucose uptake is likely to weaken their proliferative potential [41].

• Strategy 2 – The second strategy consists of decreasing the pentose phosphate pathway flux in order to hinder the synthesis of ribose, a fundamental component of nucleic acids. The rationale behind this strategy is that the most (around 75~90%) of ribose recovered from nucleic acids of certain tumour cells arrives directly or indirectly through the PPP [42,43]. Hence, inhibiting the PPP flux would result in hindering cancer cell replication [44].

• Strategy 3 – A third clinical approach may consist of inhibiting the excretion of lactic acid. Cancerous cells compete with adjacent normal cells by creating an acidic extra-cellular environment which is harmful to the non- neoplastic tissue [45]. By inhibiting lactic acid excretion (which is the main cause of the low extracellular pH in the cancer microenvironment), one would hinder one of the means by which cancerous cells invade in the pre- existing normal cell population [46,47]. At the same time, a decreased lactic acid efflux would induce the self-poisoning of cancer cells through the excess of endogenous lactic acid production [48-50].

Strategy 1: Starving cancer cells: Because we already had a reference value for the kinetic parameters (see Methods), we started to evaluate the control coefficients from sampled values only of the (unknown/uncertain) metabolite concentrations of the cancerous phenotype, in order to assess to what extent the uncertainties of the cancerous metabolic state alone were affecting the control profile of the system. By limiting the sampling process to the metabolite concentrations, we obtained one single value for each of the control coefficients in the normal metabolic state, as no quantity defining the

non-cancerous metabolic phenotype was involved in the sampling process. Conversely, in the cancerous metabolic state a distribution of values was obtained for each control coefficient, reflecting the effect that the uncertainty of the input data has on the response of the system. Figure 2 shows the distributions of the calculated selectivity coefficients of some of the enzymes in the system with respect to the uptake of glucose. The selectivity coefficients of hexokinase (Figure 2a) are entirely distributed around negative values. According to the definition of the selectivity coefficient provided in Eq. (10), this means that the magnitude of the control exerted by this enzyme on the uptake of glucose is larger in the normal phenotype than it is in the cancerous. This result seems in accordance with the fact that hexokinase (HXK) is one of the most overexpressed enzymes in many tumours [51], including breast cancer [52,53], especially in its isoform HXKII. Indeed, when the concentration (hence the activity) of a specific enzyme increases, its control is theoretically expected to decrease as a consequence of the lower degree of saturation of the enzyme with respect to its substrate [54].

Similarly, phosphofructokinase (PFK) also shows negative values of its selectivity coefficient (Figure 2b), accordingly with what one would expect on the bases of the same reasoning exposed above. Interestingly, however, the selectivity coefficient of the glucose transporter (Figure 2c) is highly positive, despite this enzyme being known to be strongly overexpressed in breast cancer [55-59]. This result, seemingly in contrast with known experimental data about enzyme expression levels, might not be in contradiction with the behaviour that the system would have *in vivo*. The overexpression of a particular enzyme, in fact, must be seen in relation with the (differential) levels of expression of all the other enzymes, as they also contribute in determining the control profile of the system. Hence overexpression of a particular enzyme does not necessarily result in a decreased of its control. The high control that the glucose transporter shows over the uptake of glucose in the cancerous phenotype might find some substantiation in a study on AS-30D and HeLa tumour cells revealing that GLT is amongst the main flux-controlling steps in both tumours (A. Marín-Hernández, R. Moreno-Sánchez and E. Saavedra, personal communication).

Another interesting result is the positive values of the selectivity coefficient of G6PDH (Figure 2d), the first enzymatic step of the pentose phosphate pathway. These positive values might well reflect the fact that the glucose uptake flux is diverted into the PPP to a much greater extent in the cancer phenotype than in the normal one. By hindering the flux through the PPP one should then elicit a greater inhibitory effect on the glucose uptake in cancer cells. This result might also suggest that G6PDH has a higher control over the PPP flux in cancer cells than it has in normal cells. We will verify this assertion later, when presenting the results obtained for the second clinical strategy (decreasing the PPP flux in order to hinder the synthesis of ribose).

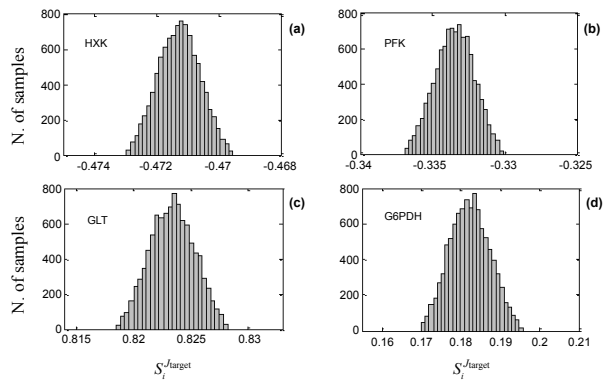

Figure 2: Selectivity coefficient distributions – Strategy 1. The selectivity coefficients are shown for HXK (a), PFK (b), GLT (c) and G6PDH (d). The results refer to a clinical strategy aimed to starve cancer cells.

A more comprehensive picture of the suitability of the different enzymes as molecular targets can be achieved by considering not only the maximal selectivity as discriminator factor, but also the criteria of minimal toxicity (or maximal safety) and maximal reliability introduced in the previous section. In order to provide a general picture of how the three criteria are met, Figure 3 shows the normalized selectivity σ_i, safety $1/\tau_i$ and reliability ρ_i plotted against each other. Only enzymes with a positive average selectivity coefficient are shown, as the others represent bad candidate drug targets. Interestingly, GLT appears to be the best candidate with respect to maximal selectivity as well as minimal toxicity (maximal safety), and it is also among the best candidates in terms of reliability.

For each enzyme we used Eq.(16) to calculate a unique score representing the overall suitability of the enzymes as putative targets, where the three criteria are simultaneously taken into account. The weight coefficients in Eq.(16) $w_\sigma = 4$, $w_\tau = 2$ and $w_\rho = 1$ in order to prioritize the maximal selectivity over the minimal toxicity (or maximal safety) and the latter over the maximal reliability. The first two columns of Table 2 list the enzymes shown in Figure 3 and their corresponding score.

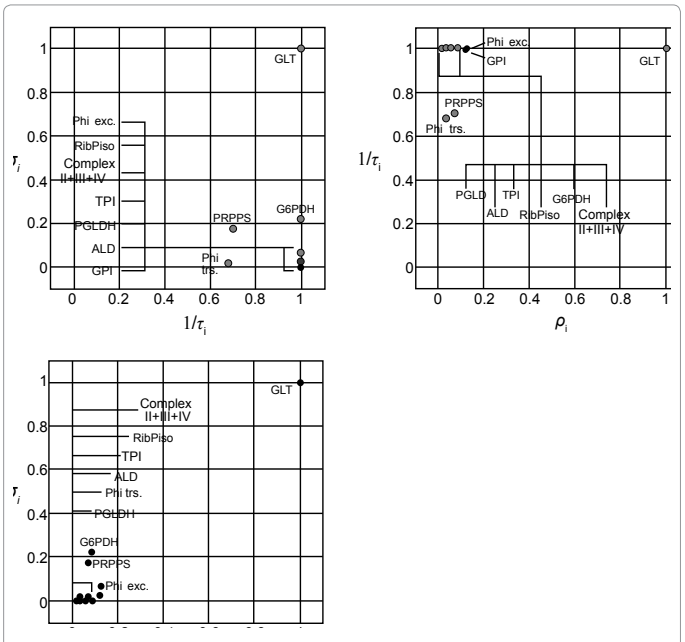

Figure 3: Normalized selectivity, safety and reliability coefficients plotted versus each other – Strategy 1. The value of the coefficients was evaluated with regard of the clinical strategy aimed to starve cancer cells.

Strategy 2: Hindering the production of ribose: The same type of analysis was repeated for a drug designed to hinder the production of ribose by inhibiting the flux through the pentose phosphate pathway. Figure 4 shows the distribution of the selectivity coefficient for some of the reaction steps in the system. The high positive values of the selectivity coefficient of G6PHD (Figure 4a) reflect the fact that the first step of PPP has a stronger control in the cancerous phenotype than in the normal, hence confirming our previous supposition. Although no comparative study has been performed yet, this result is partly corroborated by experimental studies [44] and theoretical studies [60] showing that G6PDH exerts a higher control in cancer cells over the flux of the oxidative part of PPP.

On the other hand, the selectivity coefficient of 6PGDH, the second step of pentose phosphate pathway, is distributed around very low (and negative) values (Figure 4b), meaning that the control exerted by that enzymatic step would have a very similar amplitude in both the normal and the cancerous phenotype. The glucose transporter, GLT, also shows appreciable positive values of its selectivity coefficient (Figure 4d). This is not a surprising result considering that the control exerted by GLT on the glucose uptake is higher in the cancer phenotype than in the normal. Because the glucose influx through GLT is split between PPP and the downstream steps of glycolysis, it is reasonable to expect that the positive differential control of GLT on the uptake of glucose is "echoed" in the control over the flux entering the pentose phosphate pathway. This fact makes GLT an interesting candidate target as its inhibition would elicit the desired response in the system with respect to two possible strategies of intervention, one aiming to starve cancer cells, and one aiming to hinder their replication potential by decreasing the production of ribose.

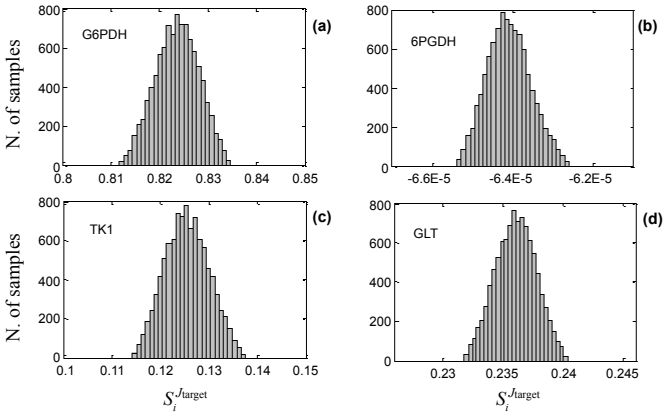

Figure 4: Selectivity coefficient distributions – Strategy 2. The selectivity coefficients are shown for G6PDH (a), 6PGDH (b), TK1 (c) and GLT (d). The results refer to a clinical strategy aimed to hinder the production of ribose.

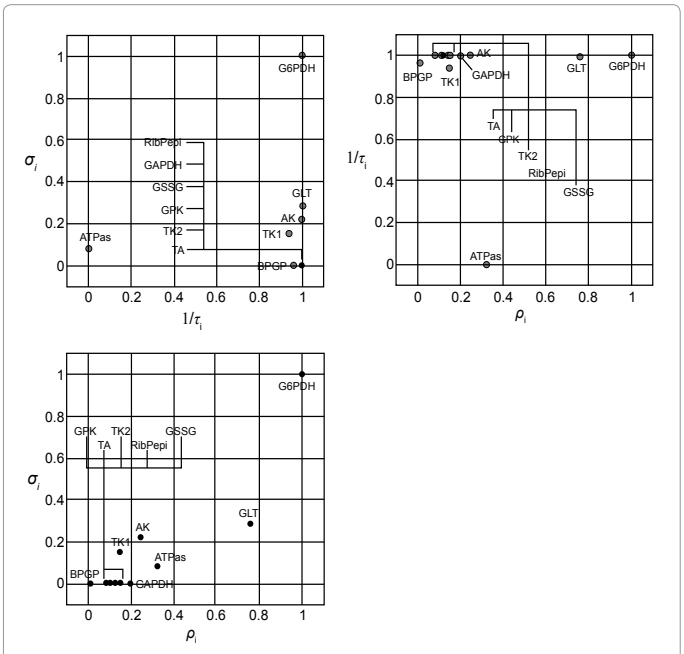

Figure 5: Normalized selectivity, safety and reliability coefficients plotted versus each other – Strategy 2. The value of the coefficients was evaluated with regard of the clinical strategy aimed to hinder ribose production.

Figure 5 shows that G6PDH is the best enzyme in terms of all the three criteria of selection. GLT might be also considered as a putative target, sharing with G6PDH (and other enzymes) the highest value of safety ($1/\tau_i$), and being the second best in terms of both selectivity and reliability. The central part of Table 2 shows the global score computed for the different enzymes through Eq. (16). The enzymes listed are the same shown in Figure 5, i.e. enzymes with a positive average selectivity coefficient $S_i^{J_{target}}$.

Strategy 3: Inhibiting the excretion of lactate: In a clinical strategy aimed to hinder the lactic acid efflux from cancer cells, one might consider to inhibit the activity of enzymes such as the lactate transporter (LCT) or the lactate dehydrogenases (denoted in Figure 1 as LDH and LDHP). Paradoxically, in our study these enzymes show very low selective coefficients (Figure 6a-6c), meaning that the control they exert on the lactic acid efflux is similar in cancer and normal cells. Although in general this represents a bad result in terms of drug selectivity, in the context of this specific clinical strategy it might not imply particularly harmful consequences. Normal cells do not rely on the fermentative pathway of glycolysis (except for muscle cells under effort), hence a drug targeting one of these enzymes might elicit the desired effect on cancer cells without compromising

Strategy 1		Strategy 2		Strategy 3	
Reaction step	**Score**	**Reaction step**	**Score**	**Reaction step**	**Score**
GLT	1.00	G6PDH	1.00	GLT	1.00
G6PDH	0.46	GLT	0.60	G6PDH	0.46
Phi exc.	0.39	AK	0.48	RibPiso	0.36
GPI	0.36	TrKet1	0.41	GPI	0.35
RibPiso	0.36	GAPDH	0.37	TPI	0.34
Comp. II+III+IV	0.35	GSSGRD	0.36	Phiexch	0.34
TPI	0.34	RibPepi	0.36	PGLDH	0.34
ALD	0.34	TrKet2	0.35	PPRPPS	0.33
PGLDH	0.34	TrAld	0.35		
PRPPS	0.33	PGK	0.35		
Phi trs.	0.24	BPGP	0.32		

Table 2: Suitability of the enzymes as drug target when only metabolite concentrations are sampled. The suitability of each enzyme as drug target is assessed with regard to the three clinical strategies described in the text. The score associated to each enzyme is computed through Eq. (16) with weight factors w_σ=4, w_τ=2 and w_ρ=1. Only enzymes with positive average selectivity are shown.

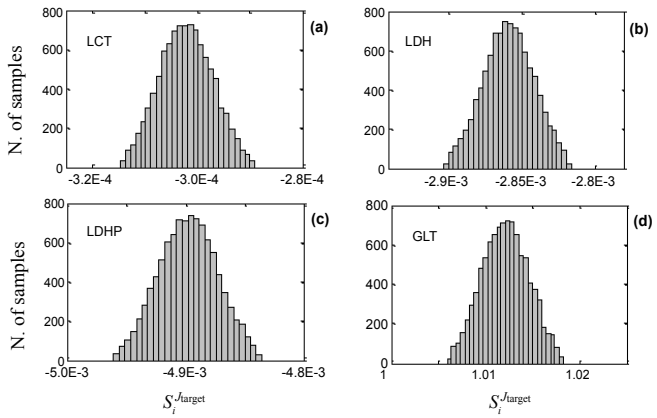

Figure 6: Selectivity coefficient distributions – Strategy 3. The selectivity coefficients are shown for LCT (a), LDH (b), LDHP (c) and GLT (d). The results refer to a clinical strategy aimed to inhibiting the excretion of lactate.

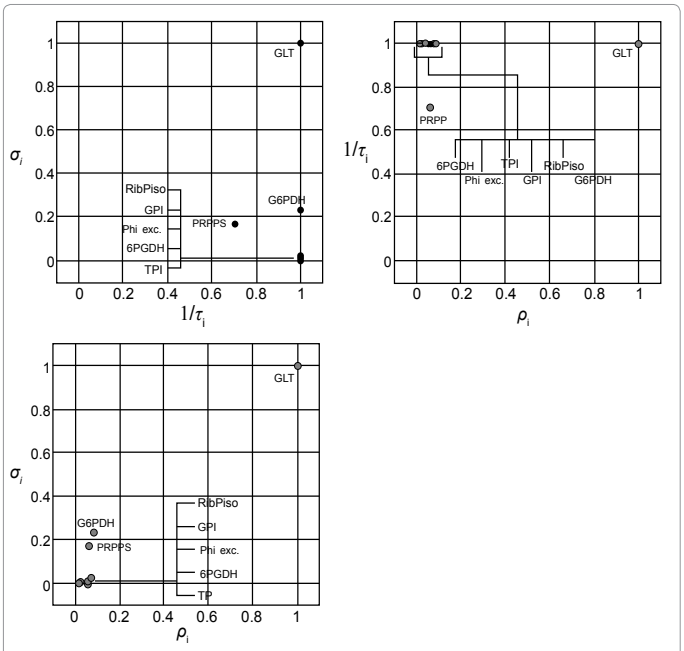

Figure 7: Normalized selectivity, safety and reliability coefficients plotted versus each other – Strategy 3. The value of the coefficients was evaluated with regard of the clinical strategy aimed to hinder the excretion of lactate.

the normal functioning of their normal counterparts. In this case, rather than the selectivity coefficient, one might be interested in the distribution of the pure flux control coefficients of LDH, LDHP and LCT. However, our data showed that for these enzymes not only the differential control (selectivity coefficient) was particularly low, but also the control coefficients corresponding to each of the metabolic states under comparison. In contrast with LCT, LDH and LDHP, a high selectivity coefficient is shown by the glucose transporter (Figure 6d). Interestingly, the values of the selectivity coefficient of GLT are higher for the efflux of lactate than for the uptake of glucose. As a consequence of targeting GLT, then, one would expect an increase in the ratio between the flux entering the TCA cycle and the glucose influx from the value of the unperturbed cancer phenotype.

From Figure 7, GLT appears to be the best putative target with respect to the criteria of highest selectivity and reliability. It is also hardly toxic, as many of the other enzyme shown in the plot. The score of the enzymes in Figure 7 is reported in the right part of Table 2.

Sampling concentrations and kinetic parameters

The same analysis performed for the three clinical strategies illustrated above was repeated by including the kinetic parameters in the set of sampled quantities. In particular, in addition to the concentrations, we sampled parameters such as Michaelis-Menten constants of inhibition/activation constants, quantifying the strength of the interaction between the enzymes with their substrates and effectors.

The effect of enlarging the set of sampled quantities consisted of spreading the distributions of the control properties over wider ranges of values. In the vast majority of cases (90%), the averages of the selectivity coefficient distributions maintained their sign. This fact implies that the main traits of the control properties of the system already emerge from the data defining the metabolic states under comparison. In particular, the qualitative behaviour of the enzymes, in terms of the differential response that their inhibition would elicit in the system between the two metabolic states, is statistically predicted to be the same independent of whether the kinetic parameters are included or not in the set of sampled quantities. However, the increased uncertainty in the definition of the model, due to the sampling of the parameters, might affect the results obtained previously in terms of the suitability of the different enzymes as putative drug targets. In Table 3 we provide the listing of the top scoring enzymes for the three different clinical strategies where the kinetic parameters were included in set of sampled quantities.

Discussion

In this paper we presented a study aimed to identify putative targets for a drug operating at the metabolic level and designed to attack breast cancer. The suitability of the different enzymes as putative targets was assessed with respect to criteria of maximal efficacy and

Strategy 1		Strategy 2		Strategy 3	
Reaction step	**Score**	**Reaction step**	**Score**	**Reaction step**	**Score**
GLT	1.00	G6PDH	1.00	GLT	1.00
Phi exc.	0.49	GLT	0.59	Phiexch	0.42
GPI	0.42	AK	0.48	GPI	0.41
ACO	0.38	TrKet1	0.40	G6PDH	0.34
G6PDH	0.35	GSSGRD	0.37	RibPiso	0.34
Phi trs.	0.35	GAPDH	0.36	TrAld	0.34
RibPiso	0.34	RibPepi	0.35	TrKet2	0.34
TPI	0.34	TrKet2	0.35	TrKet1	0.32
TrAld	0.34	TrAld	0.35		
TrKet2	0.34	PGK	0.35		
Phi trs.	0.24	BPGP	0.32		

Table 3: Suitability of the enzymes as drug targets when both metabolite concentrations and kinetic parameters are sampled.

minimal toxicity, both evaluated in terms of control coefficients. The criterion of low toxicity, in particular, requires that both the normal and the cancerous metabolic phenotypes are taken into account and their control profiles compared.

The two metabolic states (normal and cancerous) and the dynamic properties of the system were described based on currently available literature data. Unknown quantities were sampled randomly and the control properties of the system evaluated at each sampling iteration. The search for putative targets was performed with regard to three possible clinical strategies: starvation of cancer cells through inhibition of glucose uptake; hindering of cell replication by inhibition of ribose production; prevention of tumour expansion via acidification of extracellular environment by inhibiting lactate excretion. The glucose transporter (GLT) and glucose-6-phosphate dehydrogenase (G6PDH) emerged as the two best putative targets with respect to all the three clinical approaches. These results find some substantiation in previous experimental work. In particular, the inhibition of glucose-6-phosphate dehydrogenase activity has been observed to play a major role in preventing carcinogenesis [61,62], and breast cancer risk has been reported to be reduced in G6PD- deficient women [63,64].

Regarding the suitability of GLT as drug target, we could not find any confirmation in the literature specifically related to breast cancer. As mentioned above, the only partial validation of the possible relevance of GLT as drug target can be found in a study on AS-30D and HeLa tumour cells, where the role of GLT amongst the main flux-controlling steps in both tumours has been observed.

In interpreting these results, however, some considerations have to be made. For example, the normal metabolic phenotype has been described in terms of the flux pattern and metabolite concentrations of different cell types. In particular, the concentrations of cytosolic metabolites and the ratio between the glycolytic flux and the PPP flux were taken from Schuster's model of human erythrocytes [24]; on the other hand the concentration of most metabolites in mitochondria and the portion of the glycolitic flux entering the TCA cycle were retrieved by experimental data referring to skeletal muscle cells under resting condition [25]. In doing so we intended to describe the normal metabolic phenotype based, to the wider possible extent, on experimental data, hence using physiological values for the quantities defining the normal metabolic state. However, the heterogeneity of these data and the fact that they do not specifically refer to human breast cells' metabolism may affect the outcome of our study and the reliability of its predictions. For example, it is known that the glucose transporter does not exert a high control on glucose uptake in human erythrocytes [10]. This might be (or have contributed to) the reason why GLT showed a particularly high differential control between the cancerous and the normal metabolic states over influx of glucose. The experimental characterization of the metabolic phenotype in non-neoplastic human breast cells would contribute to improve the reliability of our study.

To further improve the reliability of our predictions, another aspect to be considered is the value of the equilibrium constants. In our analysis, the equilibrium constants were assumed to be known and a thermodynamically consistent set of values was obtained from [39]. We point out two possible limitations of such an assumption. First, the values of the equilibrium constants are often retrieved using computational algorithms designed to provide reasonable approximations [65-67], and they do not necessarily reflect the value of the relevant *in vivo* conditions. Experimental quantification of the free energy changes occurring in different metabolic reactions is available on repositories such as Web GCM [68], but they are currently far from covering even just the central carbon metabolism as represented in Figure 1. A second limitation is introduced by considering the same set of equilibrium constants for both the normal and the cancerous metabolic phenotypes. The value of the equilibrium constants varies depending on the specific physiological conditions, and factors such as the pH can affect it to a considerable extent [69-72]. Despite the internal pH of cancer cells is basically the same as in normal cells [33], the mitochondrial concentration of protons (which is buffered by the bigger cytosolic volume) might significantly differ in the two phenotypes, resulting in a different set of values for the equilibrium constants of mitochondrial reactions.

Regarding specifically the third clinical approach, we notice that inhibiting the excretion of lactic acid has a double effect: on one hand it prevents cancer cells from creating the hyperacidic extracellular environment by means of which they invade the normal tissue; on the other hand it results in accumulation of intracellular lactic acid with toxic effect for neoplastic cells. Depending on the rationale driving this clinical strategy, different definitions of selectivity and toxicity coefficients may be provided. If the focus is on increasing the concentration of lactic acid in transformed cells above toxic levels (rather than decreasing the acidity of the tumour micromilieu), the criteria of selectivity and toxicity might be better defined in terms of concentrations coefficients rather than flux coefficients.

As a general note on the methodology used in this work, we underline that its probabilistic nature enables us to address the abundant cases where the parameter values of the relevant *in vivo* conditions are unknown. This particularly applies to cancer, where the genetic heterogeneity of the altered cells may result in a broad range of equally plausible parameter values. The general handle provided by the virtual universality of the cancerous metabolic features (regardless of the specific genotype of the single cells) combined with the sampling of the parameter space provides us with a probabilistic overview of the suitability of the different enzymes as possible drug targets, without being biased by a specific choice of the parameter values.

A logical extension of this work could consist of determining the sensitivity of the system with respect to its different parameters. Such analysis requires that the parameters are sampled individually rather than together. This study would lead to identifying a subspace of relevant parameters upon which the system's control properties mostly depend. In addition to lowering the dimensionality of the relevant parameter space, such analysis would provide useful insights on what parameters' experimental determination would cause the largest reduction in prediction uncertainty.

Acknowledgment

We acknowledge the support of the Bioprocessing Research Industry Club (BB/I017186/1), the Doctoral Training Centre ISBML by EPSRC and BBSRC (EP/F500 009/1), the Manchester Centre of Integrative Systems Biology by BBSRC, EPSRC (BB/C0082191) and additional BBSRC support (BBD0190791). Particular thanks go to Hans Westerhoff, Kieran Smallbone and Ralf Steuer for the constructive discussions.

References

1. Warburg O, Wind F, Negelein E (1927) The Metabolism of Tumors In The Body. J Gen Physiol 8: 519-530.
2. Gottlieb E (2009) Cancer: The fat and the furious. Nature 461: 44-45.
3. Bowden AC (1999) Metabolic control analysis in biotechnology and medicine. Nat Biotechnol 17: 641-643.

4. Kitano H, Oda K, Kimura T, Matsuoka Y, Csete M, et al. (2004) Metabolic syndrome and robustness tradeoffs. Diabetes 53 Suppl 3: S6-6S15.

5. Radisavljevic Z (2004) Locus of fragility in robust breast cancer system. J Cell Biochem 92: 1020-1024.

6. Chu LH, Chen BS (2008) Comparisons of robustness and sensitivity between cancer and normal cells by microarray data. Cancer Inform 6: 165-181.

7. Hornberg JJ, Bruggeman FJ, Bakker BM, Westerhoff HV (2007) Metabolic control analysis to identify optimal drug targets. Systems Biological Approaches in Infectious Diseases Progress in Drug Research. 64: 171-189.

8. Cascante M, Boros LG, Comin-Anduix B, de Atauri P, Centelles JJ, et al. (2002) Metabolic control analysis in drug discovery and disease. Nat Biotechnol 20: 243-249.

9. Westerhoff HV, Palsson BO (2004) The evolution of molecular biology into systems biology. Nat Biotechnol 22: 1249-1252.

10. Bakker BM, Westerhoff HV, Opperdoes FR, Michels PA (2000) Metabolic control analysis of glycolysis in trypanosomes as an approach to improve selectivity and effectiveness of drugs. Mol Biochem Parasitol 106: 1-10.

11. Schellenberger J, Palsson BØ (2009) Use of randomized sampling for analysis of metabolic networks. J Biol Chem 284: 5457-5461.

12. Wang L, Hatzimanikatis V (2006) Metabolic engineering under uncertainty. I: framework development. Metab Eng 8: 133-141.

13. Wang L, Hatzimanikatis V (2006) Metabolic engineering under uncertainty—II: Analysis of yeast metabolism. Metab Eng 8: 142-159.

14. Tran LM, Rizk ML, Liao JC (2008) Ensemble modeling of metabolic networks. Biophys J 95: 5606-5617.

15. Steuer R (2007) Computational approaches to the topology, stability and dynamics of metabolic networks. Phytochemistry 68: 2139-2151.

16. Steuer R, Gross T, Selbig J, Blasius B (2006) Structural kinetic modeling of metabolic networks. Proc Natl Acad Sci U S A 103: 11868–11873.

17. Grimbs S, Selbig J, Bulik S, Holzhütter HG, Steuer R (2007) The stability and robustness of metabolic states: identifying stabilizing sites in metabolic networks. Mol Syst Biol 3: 146.

18. Murabito E, Smallbone K, Swinton J, Westerhoff HV, Steuer R (2011) A probabilistic approach to identify putative drug targets in biochemical networks. J R Soc Interface 8: 880-895.

19. Richardson AD, Yang C, Osterman A, Smith JW (2008) Central carbon metabolism in the progression of mammary carcinoma. Breast Cancer Res Treat 110: 297-307.

20. Cohen JS, Lyon RC, Chen C, et al. (1986) Differences in Phosphate Metabolite Levels in Drug- sensitive and -resistant Human Breast Cancer Cell Lines Determined by 31P Magnetic Resonance Spectroscopy. Cancer Research 46: 4087- 4090.

21. Heinrich R, Rapoport TA (1974) A linear steady-state treatment of enzymatic chains. General properties, control and effector strength. Eur J Biochem 42: 89-95.

22. Fell DA (1992) Metabolic control analysis: a survey of its theoretical and experimental development. Biochem J 286 : 313-330.

23. Reder C (1988) Metabolic control theory: a structural approach. J Theor Biol 135: 175-201.

24. Schuster R, Holzhütter HG (1995) Use of mathematical models for predicting the metabolic effect of large-scale enzyme activity alterations Application to enzyme deficiencies of red blood cells. European Journal of Biochemistry 229: 403-418.

25. Li Y, Dash RK, Kim J, Saidel GM, Cabrera ME (2009) Role of NADH/NAD+ transport activity and glycogen store on skeletal muscle energy metabolism during exercise: in silico studies. Am J Physiol Cell Physiol 296: C25-46.

26. Wu F, Yang F, Vinnakota KC, Beard DA (2007) Computer modeling of mitochondrial tricarboxylic acid cycle, oxidative phosphorylation, metabolite transport, and electrophysiology. J Biol Chem 282: 24525-24537.

27. Mogilevskaya E, Demin O, Goryanin I (2006) Kinetic model of mitochondrial Krebs cycle: unraveling the mechanism of salicylate hepatotoxic effects. J Biol Phys 32: 245-271.

28. Liebermeister W, Klipp E (2006) Bringing metabolic networks to life: convenience rate law and thermodynamic constraints. Theor Biol Med Model 3: 41.

29. de Graaf AA, Luyten PR, den Hollander JA, Heindel W, Bovée WM (1993) Lactate imaging of the human brain at 1.5 T using a double-quantum filter. Magn Reson Med 30: 231-235.

30. He Q, Shungu DC, van Zijl PC, Bhujwalla ZM, Glickson JD (1995) Single-scan in vivo lactate editing with complete lipid and water suppression by selective multiple-quantum-coherence transfer (Sel-MQC) with application to tumors. J Magn Reson B 106: 203-211.

31. Hurd RE, Freeman DM (1989) Metabolite specific proton magnetic resonance imaging. Proc Natl Acad Sci U S A 86: 4402-4406.

32. Schupp DG, Merkle H, Ellermann JM, Ke Y, Garwood M (1993) Localized detection of glioma glycolysis using edited 1H MRS. Magn Reson Med 30: 18-27.

33. Griffiths JR (1991) Are cancer cells acidic? Br J Cancer 64: 425-427.

34. Gillies RJ, Liu Z, Bhujwalla Z (1994) 31P-MRS measurements of extracellular pH of tumors using 3-aminopropylphosphonate. Am J Physiol 267: C195-203.

35. Martin GR, Jain RK (1994) Noninvasive measurement of interstitial pH profiles in normal and neoplastic tissue using fluorescence ratio imaging microscopy. Cancer Res 54: 5670-5674.

36. Stubbs M, Rodrigues L, Howe FA, Wang J, Jeong KS, et al. (1994) Metabolic consequences of a reversed pH gradient in rat tumors. Cancer Res 54: 4011-4016.

37. Wright AJ, Fellows GA, Griffiths JR, Wilson M, Bell BA, et al. (2010) Ex-vivo HRMAS of adult brain tumours: metabolite quantification and assignment of tumour biomarkers. Mol Cancer 9: 66.

38. Lee S, Palakornkule C, Domach MM, Grossmann IE (2000) Recursive MILP model for finding all the alternate optima in LP models for metabolic networks. Computers & Chemical Engineering 24: 711-716.

39. Holzhütter HG (2004) The principle of flux minimization and its application to estimate stationary fluxes in metabolic networks. Eur J Biochem 271: 2905-2922.

40. Medina RA, Owen GI (2002) Glucose transporters: expression, regulation and cancer. Biol Res 35: 9-26.

41. Harmon AW, Patel YM (2004) Naringenin inhibits glucose uptake in MCF-7 breast cancer cells: a mechanism for impaired cellular proliferation. Breast Cancer Res Treat 85: 103-110.

42. Horecker BL, Domagk G, Hiatt HH (1958) A comparison of C14-labeling patterns in deoxyribose and ribose in mammalian cells. Arch Biochem Biophys 78: 510-517.

43. Macallan DC, Fullerton CA, Neese RA, Haddock K, Park SS, et al. (1998) Measurement of cell proliferation by labeling of DNA with stable isotope-labeled glucose: studies in vitro, in animals, and in humans. Proc Natl Acad Sci U S A 95: 708-713.

44. Boren J, Montoya AR, de Atauri P, Comin-Anduix B, Cortes A, et al. (2002) Metabolic control analysis aimed at the ribose synthesis pathways of tumor cells: a new strategy for antitumor drug development. Mol Biol Rep 29: 7-12.

45. Gatenby RA, Gawlinski ET (1996) A reaction-diffusion model of cancer invasion. Cancer Res 56: 5745-5753.

46. Annibaldi A, Widmann C (2010) Glucose metabolism in cancer cells. Curr Opin Clin Nutr Metab Care 13: 466-470.

47. Shime H, Yabu M, Akazawa T, Kodama K, Matsumoto M, et al. (2008) Tumor-secreted lactic acid promotes IL-23/IL-17 proinflammatory pathway. J Immunol 180: 7175-7183.

48. Belt JA, Thomas JA, Buchsbaum RN, Racker E (1979) Inhibition of lactate transport and glycolysis in Ehrlich ascites tumor cells by bioflavonoids. Biochemistry 18: 3506-3511.

49. Kim JH, Kim SH, Alfieri AA, Young CW (1984) Quercetin, an inhibitor of lactate transport and a hyperthermic sensitizer of HeLa cells. Cancer Res 44: 102-106.

50. Mathupala SP, Colen CB, Parajuli P, Sloan AE (2007) Lactate and malignant tumors: a therapeutic target at the end stage of glycolysis. J Bioenerg Biomembr 39: 73-77.

51. Mathupala SP, Ko YH, Pedersen PL (2006) Hexokinase II: cancer's double-edged sword acting as both facilitator and gatekeeper of malignancy when bound to mitochondria. Oncogene 25: 4777-4786.

52. Brown RS, Goodman TM, Zasadny KR, Greenson JK, Wahl RL (2002) Expression of hexokinase II and Glut-1 in untreated human breast cancer. Nucl Med Biol 29: 443-453.

53. Shreeve SM, Palmieri D, Johnson MM, Aldape KD, Davis S, et al. (2008) Correlation of hexokinase-2 expression with overall survival and potential as a therapeutic target in the treatment of breast cancer brain metastases. Journal of Clinical Oncology, 2008 ASCO Annual Meeting Proceedings 26: 1005.

54. Torres NV, Mateo F, Meléndez-Hevia E, Kacser H (1986) Kinetics of metabolic pathways. A system in vitro to study the control of flux. Biochem J 234: 169-174.

55. Bos R, van Der Hoeven JJ, van Der Wall E, van Der Groep P, van Diest PJ, et al. (2002) Biologic correlates of (18)fluorodeoxyglucose uptake in human breast cancer measured by positron emission tomography. J Clin Oncol 20: 379-387.

56. Brown RS, Wahl RL (1993) Overexpression of Glut-1 glucose transporter in human breast cancer. An immunohistochemical study. Cancer 72: 2979-2985.

57. Macheda ML, Rogers S, Best JD (2005) Molecular and cellular regulation of glucose transporter (GLUT) proteins in cancer. J Cell Physiol 202: 654-662.

58. Brown RS, Wahl RL (1993) Overexpression of Glut-1 glucose transporter in human breast cancer. An immunohistochemical study. Cancer 72: 2979-2985.

59. Younes M, Lechago LV, Somoano JR, Mosharaf M, Lechago J (1996) Wide expression of the human erythrocyte glucose transporter Glut1 in human cancers. Cancer Res 56: 1164-1167.

60. Reuss M (2010) Multiscale Modeling in Cancer Therapy – Synergistic Interplay of Target Identification and Drug Delivery. In Metabolic Engineering VIII Conference. Jeju Island, Korea.

61. Schwartz AG, Whitcomb JM, Nyce JW, Lewbart ML, Pashko LL (1988) Dehydroepiandrosterone and structural analogs: a new class of cancer chemopreventive agents. Adv Cancer Res 51: 391-424.

62. Schwartz AG, Pashko LL (1993) Cancer chemoprevention with the adrenocortical steroid dehydroepiandrosterone and structural analogs. J Cell Biochem Suppl 17G: 73-79.

63. Feo F, Pirisi L, Pascale R, Daino L, Frassetto S, et al. (1984) Modulatory effect of glucose-6-phosphate dehydrogenase deficiency on benzo(a)pyrene toxicity and transforming activity for in vitro-cultured human skin fibroblasts. Cancer Research 44: 3419-3425.

64. Feo F (1988) Inhibition of initiation and promotion steps of carcinogenesis by glucose-6-phosphate dehydrogenase deficiency. In Chemical Carcinogenesis: Models and Mechanisms. Plenum Press: New York.

65. Jankowski MD, Henry CS, Broadbelt LJ, Hatzimanikatis V (2008) Group contribution method for thermodynamic analysis of complex metabolic networks. Biophys J 95: 1487-1499.

66. Alberty RA (2003) The role of water in the thermodynamics of dilute aqueous solutions. Biophys Chem 100: 183-192.

67. Henry CS, Jankowski MD, Broadbelt LJ, Hatzimanikatis V (2006) Genome-scale thermodynamic analysis of Escherichia coli metabolism. Biophys J 90: 1453-1461.

68. Jankowski MD, Henry CS, Broadbelt LJ, Hatzimanikatis V (2008) Group contribution method for thermodynamic analysis of complex metabolic networks. Biophys J 95: 1487-1499.

69. Alberty RA, Cornish-Bowden A (1993) The pH dependence of the apparent equilibrium constant, K', of a biochemical reaction. Trends Biochem Sci 18: 288-291.

70. Magnus G, Keizer J (1997) Minimal model of beta-cell mitochondrial Ca2+ handling. American Journal of Physiology, Endocrinology and Metabolism. 273: C717-C733.

71. Gunter TE, Pfeiffer DR (1990) Mechanisms by which mitochondria transport calcium. Am J Physiol 258: C755-786.

72. Wojtczak L, Zółkiewska A, Duszyński J (1986) Energy-storage capacity of the mitochondrial proton-motive force. Biochim Biophys Acta 851: 313-321.